

Behavior of Pile Foundation Subjected to Lateral Cyclic Loading in Contaminated Soils

Mahdi O. Karkush*, Mahmoud S. Abdul Kareem

Civil Engineering Department, University of Baghdad, Baghdad, Iraq

Abstract The effects of industrial wastewater on the geotechnical properties of clayey soil and the behavior of free-headed pile driven into clayey soil and subjected to lateral cyclic loading were studied in this research. The industrial wastewater discharged as by-product from an Electrical Power Plant and the intact soil samples were collected from the same region. The clayey soil samples were artificially contaminated with 10, 20, 40, and 100% (by weight) of water used in soaking process for 30 days. The results revealed that the differences in the concentration of contaminants have only slight effects on the chemical and physical properties of soil, but significant effects on the mechanical properties, including the shear strength and compression parameters. In addition, soil contamination has nonlinear effects on the lateral load-displacement relation of pile. The lateral resistance of pile decreased with increasing concentration of contaminant in the soil. The total lateral displacement of the pile head for $e/L = 0.5$ was larger than that for $e/L = 0.25$ by 22–30% under the same loads.

Keywords Industrial wastewater, Soil contamination, Geotechnical properties, Clayey soil, Cyclic loading, Lateral loading, Piles foundation

1. Introduction

In addition to the axial loads, lateral loads and moments may also act on piles. Axial downward load occur due to the gravitational force. Upward loads, lateral loads, and moments generally occur due to the natural forces such as wind, waves, and earthquake. Pile foundations are extensively used in onshore/offshore wind turbines. The piles supporting these structures are inevitably subjected to the lateral static and cyclic loading generated by forces such as the waves, current, and wind [1]. The percentage of contaminated soil has increased significantly at the sites of industrial activities with the rapid development and expansion of industries such as oil fields, refineries, factories, and electrical power stations [2].

Poulos and Davis [3] have suggested two phenomena that may contribute to the increase in the displacement of laterally loaded piles with increasing number of cycles, including cyclic soil degradation that decreases the hardness and strength of the soil. Long and Vanneste [4] improved the p-y approach by considering the effect of the number of lateral load cycles up to 50. Moreover, the use of p-y curves often fails to account for the permanent lateral displacement that accumulates with increasing numbers of cycles of loading.

Dewaikar et al. [5] studied the ultimate lateral load capacity of a flexible free-head pile in soft clay under cyclic loading with an embedded length of 30 m and eccentricity ranging from 0 to 12.5 m. They observed that the initial degradation was very high for the first few cycles. However, the ultimate lateral load capacity increased 20 times when the diameter of the pile increased five times. Haigh and Bolton [6] studied the response of a stainless steel single pile under one-way force of cyclic lateral loads. The embedded depth was 250 mm and the total length of the pile was 972 mm.

Karkush et al. [7] studied the effects of four types of contaminants (kerosene, ammonium hydroxide, lead nitrate, and copper sulfate) on the geotechnical properties of clayey soil at two different compositions (10 and 25% of dry weight of clayey soil) and found that the contaminants had different effects on the geotechnical properties of soil, depending upon the type and concentration of the contaminant. In the present study, the diverse effects of industrial wastewater on the geotechnical properties of clayey soil and the behavior of pile foundation in intact and contaminated soil under lateral cyclic loading was investigated.

2. Industrial Contamination

Industrial waste is defined as the waste generated by the manufacturing or industrial processes. The generated industrial waste includes chemical solutions, dirt and gravel, masonry and concrete, scrap metals, trash, oil, solvents,

* Corresponding author:

mahdi_karkush@fulbrightmail.org (Mahdi O. Karkush)

Published online at <http://journal.sapub.org/jce>

Copyright © 2015 Scientific & Academic Publishing. All Rights Reserved

weed grass and trees, wood and scrap lumber, and similar wastes. The industrial waste can be solid, liquid, or gaseous, and these wastes can be divided into hazardous and non-hazardous types. Industrial waste has been a problem since the industrial revolution. Hazardous industrial waste may be toxic, ignitable, corrosive, or reactive. If improperly managed, this waste can pose dangerous health and environmental risks [8] and [9].

The industrial wastewater disposed from the units of thermal electric power plant consists of chemical solvents, strong acidic, and salts. The generated quantity is about 30,000 m³/day which disposed to the soil or river, accordingly it is important to study the effects of such contaminant on the geotechnical properties of soil as well as the behavior of piles subjected to lateral cyclic loading. Iraq has several thousands of contaminated sites generated from a combination of general industrial activities, military activities, and post-conflict damage and looting [10].

3. Field Work

3.1. Material Used and Field Tests

The soil samples were obtained from the countryside of Al-Musayib city, which is located to the north of the Babylon governorate in central Iraq (UTM: 33N515276, 44E28102), while the contaminant was the industrial wastewater disposed from the Al-Musayib thermal electrical power plant. The chemical compositions of soil sample and contaminant are important to understand the behavior of contaminated soil samples. The results of chemical analysis for the assessed contaminant are given in Table 1.

Table 1. Chemical analysis of contaminant

Density kg/m ³	pH	Concentration			
		Mineral	ppm	Mineral	%
1001.3	2.65	Na	228	Zn	0.0071
		NO ₃	200	Cr	0.0001
		SO ₃	1172	Ni	0.0002
		Cl-1	180	Mg	0.0040
		CaO	ND	Fe	0.1517
		Cu	ND	K	0.00841
		Cd	ND	Ca	0.2101
		-	-	EC	0.3960

The pile model used in the present study was made using aluminum (6061) of a solid circular cross-sectional area of 19-mm diameter and 500-mm length. The properties and dimensions of the pile model are listed in Table 2. According to the criteria proposed by [1], the pile used in the present study with $L/D \geq 20$ is considered long, flexible and free-head pile. The field unit weight was 19.3 kN/m³ (ASTM D2937-00) and the natural moisture content is 32% (ASTM D2216) [11].

Table 2. Material properties and dimensions of pile model

Property	Symbol	Value
Length	e+L	500 mm
Diameter	D	19 mm
Tensile Strength	f _y	95 MPa
Ultimate Tensile Strength	f _u	110 MPa
Young Modulus	E	69 GPa
Moment of Inertia	I	6.397×10 ⁻⁹ m ⁴
Bending Stiffness	EI	4.41×10 ⁻⁴ MN.m ²

3.2. Drilling and Sampling

The soil samples were obtained from a depth of 4 m from below the natural ground level to avoid organic materials and the roots of plants and to collect samples from below the groundwater table. The ground was drilled by excavating an open hole of 10-m length and 8-m width and two types of soil samples were obtained from the hole: disturbed and undisturbed. Then, the soil samples were placed in airtight plastic containers and transported to the laboratory for further testing.

4. Laboratory Work

The disturbed and undisturbed soil samples were soaked with the contaminant for 30 days in closed plastic containers in four different percentages (10, 20, 40, and 100) by weight of the distilled water used in the soaking process. The chemical solution prepared contained a specific percentage of contaminant and distilled water sufficient to cover the soil samples and penetrate the contaminant deeply into the soil. The soil samples tested in the present study are designated as C₀, C₁, C₂, C₃, and C₄ for intact and contaminated soil samples with 10, 20, 40, and 100 %, respectively.

Table 3. Chemical analysis of soil samples

Sample	C ₀	C ₁	C ₂	C ₃	C ₄
Property					
SO ₃ (%)	0.10	0.14	0.16	0.16	0.16
Na (%)	0.10	0.12	0.13	0.14	0.14
Cl ⁻¹ (%)	0.18	0.13	0.07	0.07	0.07
TDS (%)	0.50	0.44	0.42	0.41	0.39
pH value	8.76	8.58	8.44	8.41	8.39
CaO (%)	0.10	0.11	0.11	0.11	0.11
NO ₃ (%)	0.08	0.09	0.10	0.10	0.11

Laboratory tests were conducted on the soil samples to investigate the effects of different percentages of contaminant on the chemical, physical, and mechanical properties of soil. In the X-ray diffraction tests, a small decrease in the d-spacing of the primary and secondary minerals in the intact and contaminated soil samples such as talc and montmorillonite were noted. The results of X-ray

tests revealed major reflections at 2.48, 2.88, 3.02, 3.33, 4.25, 7.15, and 14.04 Å°. This data reveals the presence of montmorillonite, kaolinite, feldspar, and dolomite as secondary minerals and quartz, calcite, and orthoclase as primary minerals. The results of chemical tests conducted according to the ASTM standards and the concentration of heavy metals measured by using the atomic absorption spectrometer (AAS) instrument are given in Table 3.

The physical properties of soil samples tested in the present work included particle size distribution (ASTM D422), liquid and plastic limits (ASTM D4318), specific gravity (BS: 1377, 1975, Test 6B) [12], and the maximum dry density and optimum moisture content (ASTM D698). The results of these tests are given in Table 4, reflecting slight changes in these properties due to soil contamination.

Table 4. Results of physical tests

Sample	C ₀	C ₁	C ₂	C ₃	C ₄
Property					
G _s	2.72	2.70	2.69	2.70	2.68
Sand (%)	4	4	4	4	4
Silt (%)	7	33	24	26	31
Clay (%)	89	63	72	70	65
USCS	CH	CH	CH	CL	CL
LL (%)	56	54	53	49	48
PL (%)	23	24	24	25	26
PI (%)	33	30	29	24	22
γ _{d,max} (kN/m ³)	16.96	16.90	16.70	16.64	16.60
ω _{opt} (%)	19.0	20.0	22.0	22.7	23.0

The results of one-dimension compression tests conducted on intact undisturbed and contaminated remolded soil samples according to ASTM (D2435) are given in Table 5. In addition, the results of shear strength parameters measured by unconfined compression test (UCT) (ASTM D2166), direct shear test (DST) (ASTM D3080-72), and vane shear test (VST) (ASTM D4648) are given in Table 5.

Table 5. Results of consolidation tests

Sample	C ₀	C ₁	C ₂	C ₃	C ₄
Property					
c _v × 10 ⁻² (cm ² /sec)	0.18	0.19	0.22	0.24	0.25
k × 10 ⁻⁸ (cm/sec)	1.543	1.66	2.195	2.49	2.879
e ₀	0.86	0.83	0.81	0.81	0.8
e _f	0.65	0.61	0.58	0.57	0.54
m _v × 10 ⁻⁵ (m ² /kN)	8.367	8.54	9.726	10.16	11.4
D × 10 ³ (kN/m ²)	11.95	11.71	10.28	9.84	8.77

The results of modulus of subgrade reaction (K_s) measured by plate loading test according to the ASTM D1196 on two square steel plates (dimensions 150 × 80 mm and 125 × 125 × 80 mm) are given in Table 7. The difference in the mechanical properties of soil samples were

significant with different percentages of industrial wastewater used for contamination.

Table 6. Results of shear strength tests

Sample	UCT		DST		VST
	c _u kN/m ²	E MN/m ²	c _u kN/m ²	φ degree	c _u kN/m ²
C ₀	90	9.50	78	23.8	102
C ₁	84	8.75	74	22.5	94
C ₂	79	8.00	71	21	87
C ₃	72	7.80	66	20	79
C ₄	63	6.20	57	17	66

Table 7. Results of plate loading tests

Sample		C ₀	C ₁	C ₂	C ₃	C ₄
Property						
K _s MN/m ³	From 150 mm plate	33.8	32.3	29.23	26.92	24.62
	From 125 mm plate	34.6	32.3	30.77	27.70	23.00

4.1. Pile Loading Model

The pile model used in the present study is shown in Figure 1, and it consists of a steel container, a pile fixing tool, a dial gauge fixing tool, and a load application system. The steel container was made of steel plates of 2.5-mm thickness with internal dimensions of 700-mm length, 500-mm width, and 500-mm height. The top of the box had six holes, of which four (8-mm diameter) were used in the fixing of pile during the driving process into the soil to ensure verticality of the inserted pile, and the other two holes (10-mm diameter) were used to fix the dial gauge. In the right side of box, two angles of 50 × 50 × 300 mm were welded to the container to fix the loading system “hydraulic pressure” by two screws of 6-mm diameter.

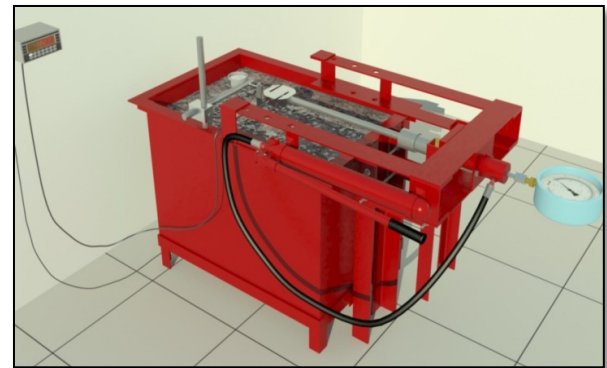


Figure 1. Laterally pile loading model

The loading system consists of a 10000-kg hydraulic pressure jack, 250-kg pressure gauge, type S load cell (500-kg capacity, output rate 2.001 mv/V), and digital weighing indicator (SI 4010). The operating temperatures range was -10°C to 40°C.

The procedure of testing can be summarized as follows:

- 1) Preparing the pile model, soil sample, and the necessary prescribed instruments and equipment;
- 2) Adding the soil in six layers (each 80-mm thick) with tamping to reach the field unit weight and moisture content;
- 3) Inserting the pile into the soil to the required embedded depth;
- 4) Installation of the loading system (hydraulic pressure jack, pressure gauge, load cell, and digital weighing indicator) and dial gauge at the free-head of the pile;
- 5) Soaking the soil sample in distilled water to cover the soil sample in the box. For intact soil, only distilled water was used, while a chemical solution (distilled water mixed with industrial wastewater in four concentrations [10, 20, 40, and 100%] by weight of water) was used for soaking the contaminated soil samples. Then, the soil sample was soaked for 6 h before starting the loading process;
- 6) The lateral loading process by started by applying incremental loads of (0.5, 1, 2, 4, 8, 10, 12, 14, 16, 18, 20, 24, 28, 32, 36, 40, and 45) kg. The rate of loading cycle was 1 cycle/min for each load increment in both the loading and unloading stages;
- 7) The readings of dial gauge during loading (horizontal displacement) and during unloading (permanent displacement) was recorded.

5. Results and Discussions

The effects of different percentages of contamination on the horizontal total and permanent displacement of head pile under lateral cyclic loads at two different ratios of eccentricity to embedded length ($e/L = 0.25$ and $e/L = 0.5$) was studied. The variation in the total and permanent displacements with lateral cyclic loading for $e/L = 0.25$ and $e/L = 0.5$ are illustrated in Figures 2 to 11.

In addition, the variation in the total displacement with a lateral load at the 1st and 100th cycles of loading is shown in Figures 12 to 15. The lateral load capacity of pile after 100th cycles decreased by 5, 11, 17, and 36% for $e/L = 0.25$ and decreased by 6, 12.5, 18, and 31% for $e/L = 0.5$, which decreased with the increasing percentage of contamination due to decreasing soil strength and cohesion. The increase in eccentricity to embedded length ratio caused a decrease in the lateral load capacity of pile; this decrease resulted from increase in the ultimate moment on the pile head, which causes increase in the horizontal displacement and decrease in the soil strength around the pile shaft. Comparison of the lateral load capacity with e/L is given in Table 8, which shows a reduction of 25–30% with increasing e/L from 0.25 to 0.5. Generally, the ratio of permanent to total displacement at 100th of cycles of loading ranged between 21 and 33%, as shown in Table 9.

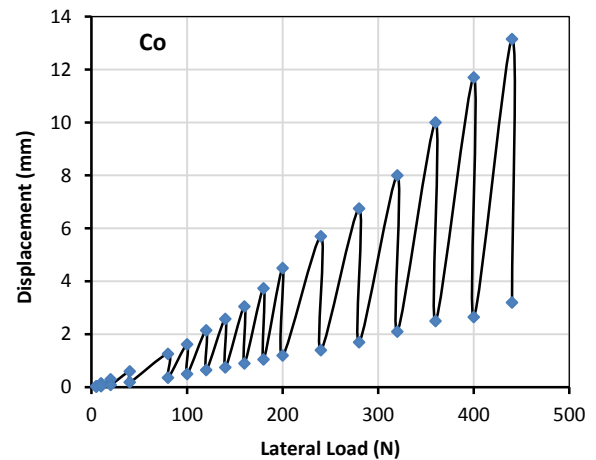


Figure 2. Displacement versus lateral load for C_0 and $e/L = 0.25$

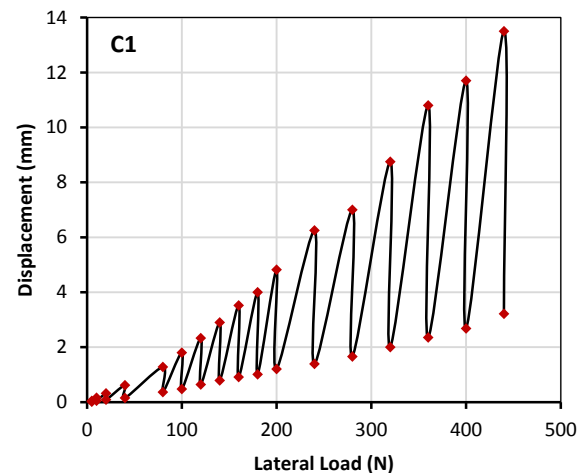


Figure 3. Displacement versus lateral load for C_1 and $e/L = 0.25$

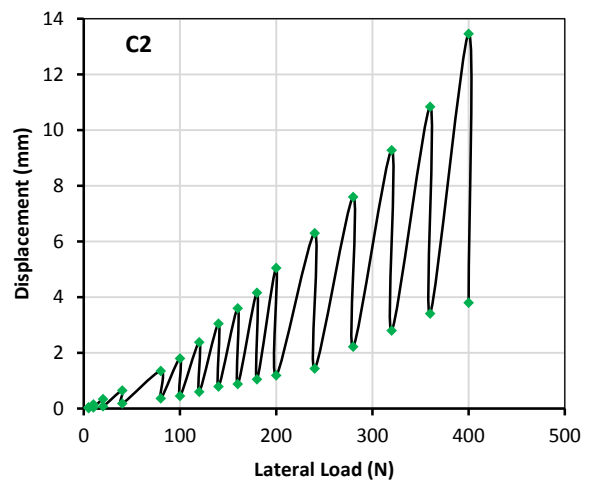
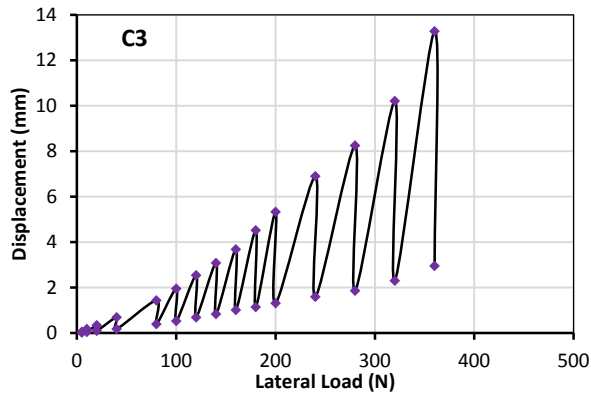
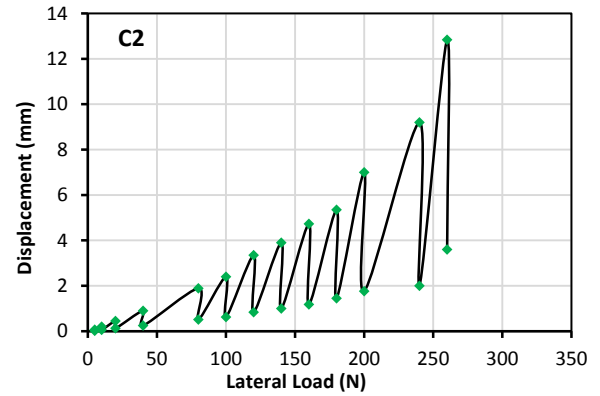
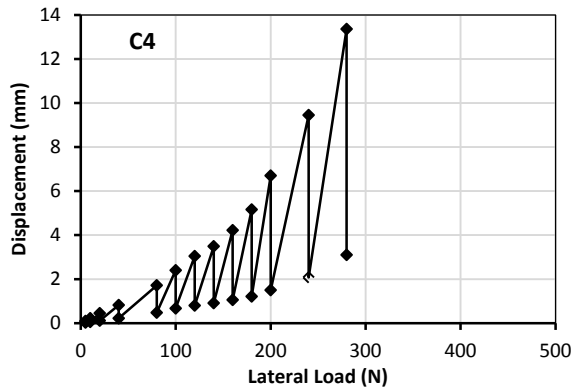
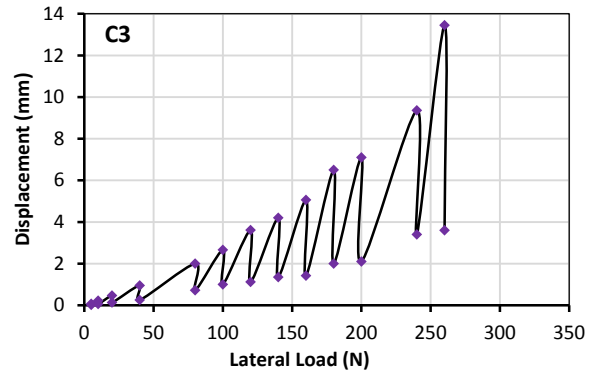
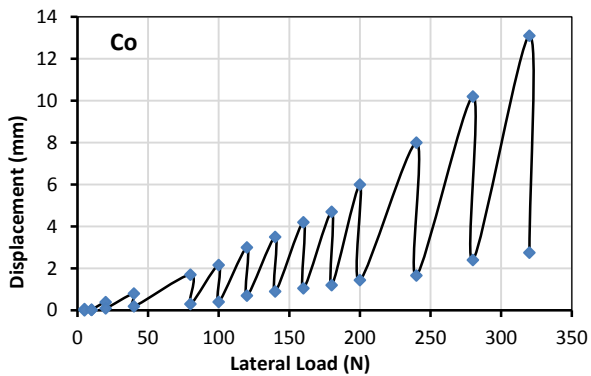
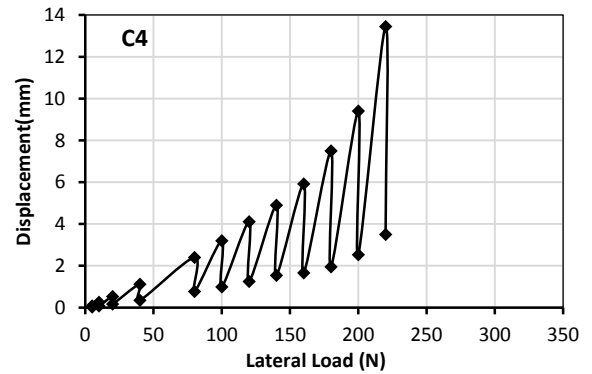
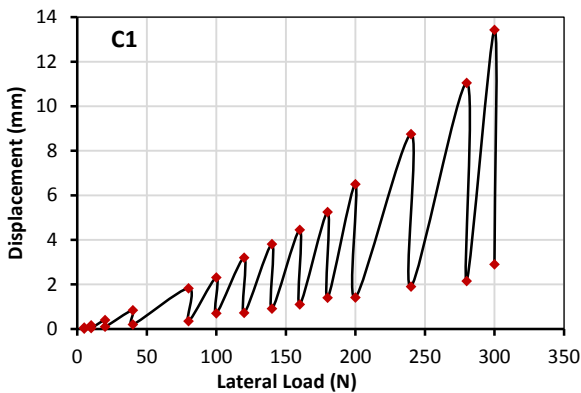
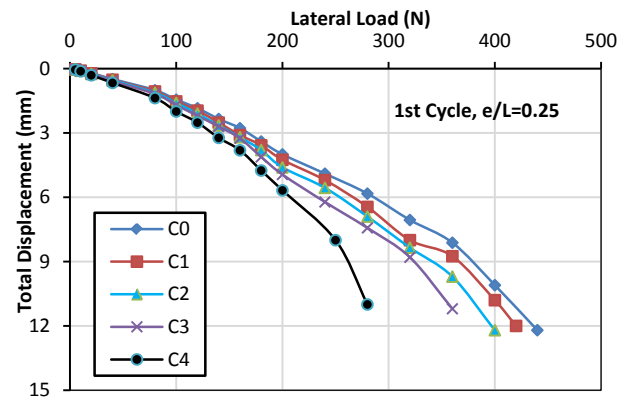


Figure 4. Displacement versus lateral load for C_2 and $e/L = 0.25$

Figure 5. Displacement versus lateral load for C_3 and $e/L = 0.25$ Figure 9. Displacement versus lateral load for C_2 and $e/L = 0.5$ Figure 6. Displacement versus lateral load for C_4 and $e/L = 0.25$ Figure 10. Displacement versus lateral load for C_3 and $e/L = 0.5$ Figure 7. Displacement versus lateral load for C_0 and $e/L = 0.5$ Figure 11. Displacement versus lateral load for C_4 and $e/L = 0.5$ Figure 8. Displacement versus lateral load for C_1 and $e/L = 0.5$ Figure 12. Total displacement versus lateral load at $N = 1$ cycle

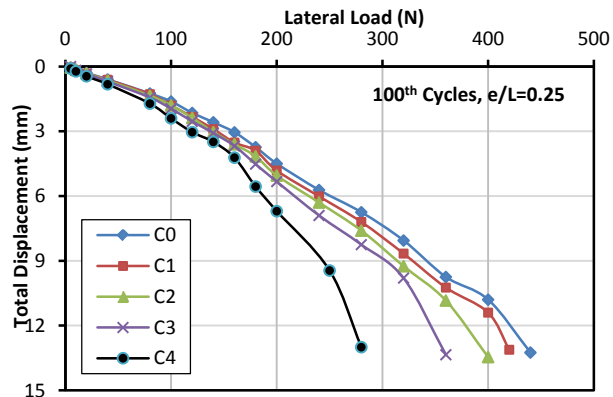


Figure 13. Total displacement versus lateral load at N = 100 cycles

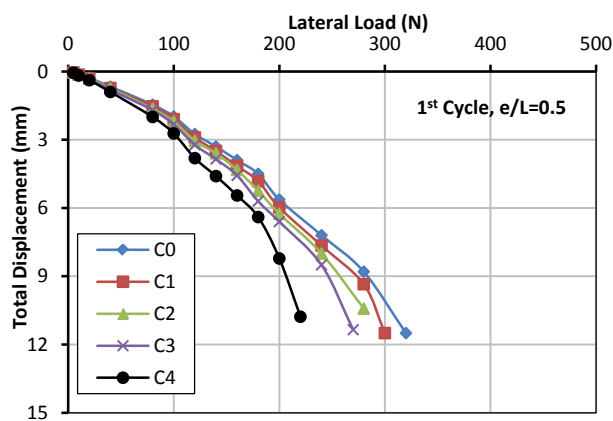


Figure 14. Total displacement versus lateral load at N = 1 cycle

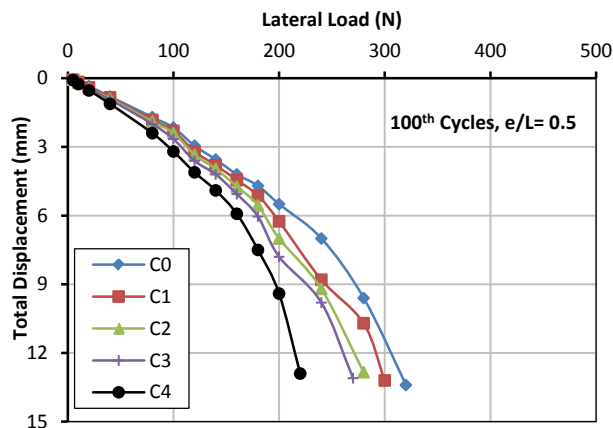


Figure 15. Total displacement versus lateral load at N = 100 cycles

Table 8. The variation of lateral load capacity with (e/L) ratio

Soil Sample	Ultimate Lateral Load (N)		$(e/L)_2 / (e/L)_1$
	$(e/L)_1 = 0.25$	$(e/L)_2 = 0.5$	
C ₀	440	320	0.72
C ₁	420	300	0.71
C ₂	400	280	0.70
C ₃	360	270	0.75
C ₄	280	220	0.78

Table 9. The ratio of permanent to the total displacement

Soil Sample	Ratio of permanent to total displacement, %	
	$e/L = 0.25$	$e/L = 0.5$
C ₀	27	21
C ₁	28	21
C ₂	30	24
C ₃	31	27
C ₄	33	27

6. Conclusions

The industrial wastewater disposed from the thermal electric power plant had diverse effects on the geotechnical properties of clayey soil obtained from the same city. This diversity ranged from slight for some soil properties to significant for other soil properties. In addition, the contamination has significant effects on the ultimate capacity of a single pile subjected to lateral cyclic loading. The conclusions of the study can be summarized as follows:

1. If the loading rate is not uniform, the displacement may be greater or less than the previous displacement because the soil needs some time to recover its resistance;
2. Cracks were noticed in the soil at the front side of pile, whereas the clay at the rear of the pile suffered from heave, which continue to produce a gap around the pile. This observation agrees with the result presented by [13];
3. The lateral bearing capacity of the pile decreased by 5, 11, 17, and 36% for $e/L = 0.25$ and decreased by 6, 12.5, 18, and 31% for $e/L = 0.5$ with increase in the percentage of contamination in soil;
4. The ratio of permanent displacement to the total displacement increased by 21–33% with increase in the percentage of contamination in soil.

REFERENCES

- [1] M. J. Tomlinson, 1994, Pile design and construction practice, 4th Edition, View Point Publication, London.
- [2] USEPA, Pump-and-treat ground-water remediation: a guide for decision makers and practitioners, EPA/625/R-95/005, Office of Research and Development, Washington, D.C., 1986.
- [3] H. G. Poulos and E. H. Davis, 1980, Pile foundation analysis and design, John Wiley & Sons, Hoboken, New York.
- [4] J. H. Long and G. Vannest, Effect of cyclic lateral loads on piles in sand, Journal of Geotechnical Engineering, ASCE, 120 (1), 225–243, 1994.
- [5] D. M. Dewaikar, S. V. Padmavathi and R. S. Salimath, 2008, Ultimate lateral load of a pile in soft clay under cyclic loading,

- 12th International Conference of International Association for Computer Methods and Advances in Geomechanics, 3498–3507.
- [6] S. K. Haigh and M. D. Bolton, 2012, Centrifuge modeling of mono pile under cyclic lateral loads, 7th International Conference on Physical Modeling in Geotechnics, Zurich, 2, 965–970.
- [7] M. O. Karkush, A. T. Zaboony and H. M. Hussien, 2013, Studying the effects of contamination on the geotechnical properties of clayey soil, Proc., Coupled Phenomena in Environmental Geotechnics, Taylor & Francis Group, London, 599–607.
- [8] R. K. Rowe, 2001, Geotechnical and geoenvironmental engineering handbook, Springer Science and Business Media, New York.
- [9] H. D. Sharma and K. R. Reddy, 2004, Geoenvironmental engineering: site remediation, waste containment, and emerging waste management technologies, John Wiley & Sons, Hoboken, New Jersey.
- [10] UNEP Report, 2005, Assessment of environmental “hot spots” in Iraq, Report ISBN 92-807-2650-1.
- [11] Annual book of ASTM standards, Soil and Rock; Building; Stone; Peats, 2003.
- [12] British Standards, BS1377, Methods of testing for civil engineering purpose, British Standards Institution, London, 1976.
- [13] S. Basack, 2009, Response of vertical pile group subjected to horizontal cyclic load in soft clay, Latin American Journal of Solids and Structures, 7, 91–103.